



ELSEVIER

Available online at [www.sciencedirect.com](http://www.sciencedirect.com)

SCIENCE @ DIRECT®

Journal of Petroleum Science and Engineering xx (2005) xxx–xxx

**JOURNAL OF  
PETROLEUM  
SCIENCE &  
ENGINEERING**
[www.elsevier.com/locate/petrol](http://www.elsevier.com/locate/petrol)

1

## 2 Correction of basic equations for deep bed filtration with dispersion

3 J.E. Altoé F.<sup>a</sup>, P. Bedrikovetsky<sup>a,\*</sup>, A.G. Siqueira<sup>b</sup>, A.L.S. de Souza<sup>b</sup>, F.S. Shecaira<sup>b</sup>

4 <sup>a</sup> Department of Petroleum Exploration and Production Engineering, North Fluminense State University Lenep/UENF,  
5 Rod. Amaral Peixoto, km 163 – Av. Brenand, s/n° Imboacica – Macaé, RJ 27.925-310, Brazil

6 <sup>b</sup> Petrobras/Cenpes, Cidade Universitaria Q.7, Ilha Do Fundão, 21949-900 – Rio De Janeiro — RJ, Brazil

7

Accepted 4 November 2005

8

### 9 Abstract

10 Deep bed filtration of particle suspensions in porous media occurs during water injection into oil reservoirs, drilling fluid  
11 invasion into reservoir productive zones, fines migration in oil fields, bacteria, virus or contaminant transport in groundwater,  
12 industrial filtering, etc. The basic features of the process are advective and dispersive particle transport and particle capture by the  
13 porous medium.

14 Particle transport in porous media is determined by advective flow of carrier water and by hydrodynamic dispersion in micro-  
15 heterogeneous media. Thus, the particle flux is the sum of advective and dispersive fluxes. Transport of particles in porous media is  
16 described by an advection–diffusion equation and by a kinetic equation of particle capture. Conventional models for deep bed  
17 filtration take into account hydrodynamic particle dispersion in the mass balance equation but do not consider the effect of  
18 dispersive flux on retention kinetics.

19 In the present study, a model for deep bed filtration with particle size exclusion taking into account particle hydrodynamic  
20 dispersion in both mass balance and retention kinetics equations is proposed. Analytical solutions are obtained for flows in infinite  
21 and semi-infinite reservoirs and in finite porous columns. The physical interpretation of the steady-state flow regimes described by  
22 the proposed and the traditional models favours the former.

23 Comparative matching of experimental data on particle transport in porous columns by the two models is performed for two sets  
24 of laboratory data.

25 © 2005 Published by Elsevier B.V.

26 *Keywords:* Deep bed filtration; Dispersion; Suspension; Governing equations; Modelling; Porous media; Emulsion

27

### 28 1. Introduction

29 Severe injectivity decline during sea/produced water  
30 injection is a serious problem in offshore waterflood  
31 projects. The permeability impairment occurs due to  
32 capture of particles from injected water by the rock.

33 The reliable modelling-based prediction of injectivity  
34 decline is important for the injected-water-treatment  
35 design, for injected water management (injection of  
36 sea- or produced water, their combinations, water fil-  
37 tering), etc.

38 The formation damage induced by penetration of  
39 drilling fluid into a reservoir also occurs due to particle  
40 capture by rocks and consequent permeability reduc-  
41 tion. Other petroleum applications include sand produc-  
42 tion control, fines migration and deep bed filtration in  
43 gravel packs.

\* Corresponding author. Tel.: +55 22 27733391; fax: +55 22 27736565.

E-mail addresses: [pavel@lenep.uenf.br](mailto:pavel@lenep.uenf.br), [pavel.russia@globo.com](mailto:pavel.russia@globo.com) (P. Bedrikovetsky).

The basic equations for deep bed filtration taking into account advective particle transport and the kinetics of particle retention, and neglecting hydrodynamic dispersion have been derived essentially following the filtration equation proposed by Iwasaki (1937). A number of predictive models have been presented in the literature (Sharma and Yortsos, 1987a,b,c; Elimelech et al., 1995; Tiab and Donaldson, 1996; Khilar and Fogler, 1998; Logan, 2001). The equations allow for various analytical solutions, which have been used for the treatment of laboratory data and for prediction of porous media contamination and clogging (Herzig et al., 1970; Pang and Sharma, 1994; Wennberg and Sharma, 1997; Bedrikovetsky et al., 2001, 2002).

However, particle dispersion in heterogeneous porous media is important for both small and large scales (Lake, 1989; Jensen et al., 1997). The typical core sizes in laboratory experiments are small, and hence the Peclet number is relatively high. The typical dispersivity values for large formation scales are high, and consequently the Peclet number may also take high values. The Peclet number for either situation may amount up to 10–20.

The effect of dispersion on deep bed filtration is particularly important near to wells, where the dispersivity may already arise to the bed scale, and the formation damage occurs in one two-meter neighbourhood.

Therefore, several deep bed filtration studies take into account dispersion of particles (Grolimund et al., 1998; Kretschmar et al., 1997; Bolster et al., 1998; Unice and Logan, 2000; Logan, 2001; Tufenkji et al., 2003). A detailed description of such early work is presented in the review paper by Herzig et al. (1970). The models developed account for particle dispersion in the mass balance for particles but do not consider the dispersion flux contribution to the retention kinetics.

In the present study, the proposed deep bed filtration model takes into account dispersion in both the equation of mass balance and in that of capture kinetics. Several analytical models for constant filtration coefficient and for dynamic blocking filtration coefficient have been developed. If compared with the traditional model, the proposed model exhibits more realistic physics behaviour. The difference between the traditional and proposed model is significant for small Peclet numbers.

The structure of the paper is as follows. In Section 2 we formulate the corrected model for deep bed filtration of particulate suspensions in porous media accounting for hydrodynamic dispersion of suspended particles. The dispersion-free deep bed filtration model is presented in Section 3 as a particulate case of the general

system with dispersion. The analytical models for flow in infinite and semi-infinite reservoirs for constant filtration coefficient are presented in Sections 4 and 5, respectively. An analytical solution for deep bed filtration in semi-infinite reservoirs with the fixed inlet concentration is given in Section 6. Analytical steady state solution for laboratory coreflood is discussed in Section 7. The analytical models allow for laboratory data treatment (Section 8). Travelling wave flow regimes for dynamic blocking filtration coefficient are described in Section 9. In Section 10, three dimensional equations for deep bed filtration with dispersion are derived. Mathematical details of the derivations are presented in Appendices. Dimensionless form of governing equations and initial-boundary conditions are given in Appendix A. The transient solutions for flow in infinite and semi-infinite reservoirs and constant filtration coefficient are derived in Appendices B, C and D. Appendix E contains derivations for steady state solution in a finite core. Appendix F contains derivations for travelling wave flow.

## 2. Model formulation

Let us derive governing equations for deep bed filtration taking into account particle dispersion. The usual assumptions of constant suspension density and porosity for low particle concentrations are adopted. The balance equation for suspended and retained particles (Iwasaki, 1937; Herzig et al., 1970) is:

$$\frac{\partial}{\partial t}(\phi c + \sigma) + \frac{\partial q}{\partial x} = 0 \quad (1)$$

Here, the concentration  $c$  is a number of suspended particles per unit volume of the fluid, and the retained particle concentration  $\sigma$  is a number of captured particles per unit volume of the rock.

The particle flux  $q$  consists of the advective and dispersive components:

$$q = Uc - D \frac{\partial c}{\partial x} \quad (2)$$

$$D = \alpha_D U \quad (3)$$

Here the dispersion coefficient  $D$  is assumed to be proportional to the flow velocity  $U$ , and the proportionality coefficient  $\alpha_D$  is called the longitudinal dispersivity (Lake, 1989; Nikolaevskij, 1990; Sorbie, 1991).

Let us consider the following physical model for the size exclusion particle capture in porous media (Santos and Bedrikovetsky, 2005). Particles are not captured during flow through the pore system, but there is a

143 sequence of particle capturing sieves perpendicular to  
144 the flow direction. The probability for a particle to be  
145 captured is equal to  $\lambda l$  ( $l$  is the distance between the  
146 sieves), and that to pass through is  $1 - \lambda l$ . In other  
147 words, after particles pass the distance  $l$ , their flux  
148 reduces  $1 - \lambda l$  times.

149 So, the so called filtration coefficient  $\lambda$  is determined  
150 through the fraction  $\lambda l$  of the particle flux that remains  
151 in porous media during flow along the distance  $l$  (Iwa-  
152 saki, 1937). The filtration coefficient  $\lambda$  is the probabil-  
153 ity for particle to be captured during the flow over the  
154 unit distance; its dimension is  $L^{-1}$ .

155 Following the probabilistic interpretation of filtra-  
156 tion coefficient, Herzig et al. (1970) have calculated  
157 the number of captured particles per unit time per unit  
158 volume during advective flow. Let us calculate the  
159 deposition rate for advective–dispersive flow. The  
160 number of particles crossing sieve during time  $\Delta t$  is  
161 equal to  $qA\Delta t$ , where  $A$  is a cross section area. The  
162 particles move along the distance  $U\Delta t/\phi$  during this  
163 time, here  $\phi$  is the porosity. The probability for  
164 particle to be captured is  $\lambda U\Delta t/\phi$ . Particle retention  
165 takes place in the volume  $AU\Delta t/\phi$ . The deposition  
166 rate is

$$\frac{\Delta\sigma}{\Delta t} = \frac{(qA\Delta t)(\lambda U\Delta t/\phi)}{(AU\Delta t/\phi)\Delta t} = \lambda q$$

168 So, the interpretation of the capture rate in terms of  
170 probability for the particle capture in elementary refer-  
171 ence volume implies that the capture rate is proportion-  
172 al to the total particle flux (Eq. (2)) rather than just to its  
173 advective component.

174 From now on we assume that the particle capture  
175 rate is proportional to the overall particle flux (first-  
176 order particle retention kinetics):

$$\frac{\partial\sigma}{\partial t} = \lambda(\sigma)q \quad (4)$$

178 Here the filtration coefficient  $\lambda(\sigma)$  is a function of  
180 retained concentration  $\sigma$ . Particle deposition changes  
181 the pore space geometry and, consequently, the condi-  
182 tions for size exclusion capture, so the deposition rate  
183 should be retained-concentration-dependent.

184 Fig. 1 illustrates size exclusion capture of particles  
185 — a pore captures a particle if the particle size exceeds  
186 the pore size, otherwise the particle passes through the  
187 pore. Therefore, the capture rate must be proportional to  
188 the total particle flux. A particle is captured by a pore  
189 regardless of whether the advective or dispersive flux  
190 has brought the particle to the pore.

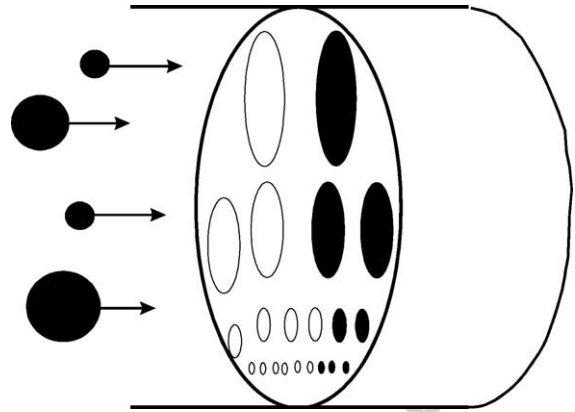


Fig. 1. Schema for particle capture by size exclusion in deep bed filtration.

The same applies to bridging build-up and to the  
consequent particle capture (Payatakes et al., 1974;  
Elimelech et al., 1995).

It is worth mentioning that usually size exclusion is  
not dominant in virus and bacteria capture during their  
flow in porous media. The retention mainly happens  
due to sorption (Kuhnen et al., 2000). In this case, the  
authors assume that the deposition rate is proportional  
to suspended concentration only. The proportionality  
coefficient dimension is  $1/T$ , i.e. the proportionality  
coefficient is a probability for particle to be captured  
during the unitary time. In this case, neither hydrody-  
namic dispersion nor advective velocity enters in the  
capture rate expression.

The same applies to chemical reactions and dissolu-  
tion in porous media (Kechagia et al., 2002).

Many experiments show that during the particle  
suspension flow in porous media, the particle capture  
rate rapidly decreases as particles start to accumulate on  
the collectors; the retention stops when the retained  
concentration reaches some critical value (Elimelech  
et al., 1995; Kuhnen et al., 2000). This phenomenon  
is called blocking. It can be explained by decrease of  
the number of vacancies for further retention during the  
retention process.

For example, if the injected particle sizes are compa-  
rable with pore throats sizes, the particles are captured  
by the pore size exclusion. Consider a wide throat size  
distribution, and injection of particles with intermediate  
sizes. Particles are captured in smaller pores. When all  
small pores are filled, the suspension flows through thick  
throats, and the particles are not captured any more.

Hereafter the following features of the filtration  
blocking coefficient  $\lambda(\sigma)$  are assumed:

$$0 < \sigma < \sigma_m : \lambda(\sigma) > 0; \sigma \geq \sigma_m : \lambda(\sigma) = 0 \quad (5)$$

226 The important particular case of Eq. (5) is the linear  
227 filtration coefficient

$$\lambda(\sigma) = \lambda_0(1 - b\sigma) \quad (6)$$

228 so called Langmuir blocking function (Kuhnen et al.,  
230 2000). It is typical where the capture is realized by a  
231 mono-layer adsorption.

232 This case corresponds to the situation where one  
233 vacancy can be filled by one particle. So, retention of  
234 some particles results in filling of the same number of  
235 vacancies, i.e. the total of deposited particle concentra-  
236 tion  $\sigma(x, t)$  and the vacant pore concentration  $h(x, t)$  is  
237 equal to initial concentration of vacancies  $h(x, 0)$ :

$$h(x, t) = h(x, 0) - \sigma(x, t) \quad (7)$$

238 The capture rate is proportional to the product of  
241 particle flux and vacancy concentration (acting mass  
242 law). Using Eq. (7), we obtain:

$$\frac{\partial \sigma}{\partial t} = \lambda_0 \left( 1 - \frac{\sigma}{h(x, 0)} \right) q \quad (8)$$

243 The filtration function  $\lambda(\sigma)$  depends on porous media  
246 structure. Therefore, for heterogeneous porous media  
247 where initial vacancy concentration depends on  $x$ , the  
248 filtration function is  $x$ -dependent:  $\lambda = \lambda(\sigma, x)$ . Further in  
249 the paper we assume a uniform initial vacancy concentra-  
250 tion and use the dependency  $\lambda = \lambda(\sigma)$ .

251 So, the Langmuir linear blocking function (Eq. (6))  
252 corresponds to “one particle – one pore” kinetics [Eq.  
253 (8)]. The comparison of formulae Eqs. (8) and (4)  
254 results in Eq. (6).

255 If  $\lambda_0$  in Eq. (8) is also a function of  $\sigma$ , the blocking  
256 filtration coefficient  $\lambda(\sigma)$  is non-linear.

257 Darcy’s law for suspension flow in porous media  
258 includes the effect of permeability decline during par-  
259 ticle retention:

$$U = - \frac{k_0 k(\sigma)}{\mu} \frac{\partial p}{\partial x} \quad (9)$$

$$k(\sigma) = \frac{1}{1 + \beta \sigma} \quad (10)$$

260  
261 Here  $k(\sigma)$  is called the permeability reduction function,  
264 and  $\beta$  is the formation damage coefficient.

265 Eqs. (1), (2), (4) and (9) form a closed system of four  
266 equations that govern the colloid filtration with size  
267 exclusion particle capture in porous media. The  
268 unknowns are suspended concentration  $c$ , deposited  
269  $\sigma$ , particle flux  $q$  and pressure  $p$ .

270 The independence of the filtration and dispersion  
271 coefficients of pressure allows separation of Eqs. (1),  
272 (2) and (4) from Eq. (9), which means that the sus-  
273 pended and retained concentrations and the particle flux

274 can be found from the system of Eqs. (1), (2) and (4)  
275 and then the pressure distribution can be found from  
276 Eq. (9).

277 Form of the system of governing equations in  
278 non-dimensional co-ordinates is presented in Appen-  
279 dix A, (Eqs. (A-2)–(A-5)). The system contains the  
280 dimensionless parameter  $\varepsilon_D$  that is the inverse to the  
281 Peclet number; it is equal to the dispersion-to-advective  
282 flux ratio (Nikolaevskij, 1990). From Eq. (3) it follows  
283 that:

$$\varepsilon_D = \frac{1}{\text{Pe}} = \frac{D}{LU} = \frac{\alpha_D}{L} \quad (11)$$

284 The dispersion–advective ratio  $\varepsilon_D$  is equal to the ratio  
287 between the micro heterogeneity size  $\alpha_D$  (dispersivity)  
288 and the reference size of the boundary problem  $L$ .

289 Let us estimate the contribution of dispersion to the  
290 total particle flux (Eq. (2)). In the majority of papers,  
291 deep bed filtration model has been modelled under the  
292 laboratory floods conditions, where homogeneous sand  
293 columns are employed (Elimelech et al., 1995; Unice  
294 and Logan, 2000; Tufenkji et al., 2003). On the core  
295 scale in homogeneous cores, we have  $L \sim 0.1$  m,  
296  $\alpha_D \sim 0.001$  m,  $\varepsilon_D \sim 0.01$ , and hence the dispersion can  
297 be neglected. In natural heterogeneous cores,  $\varepsilon_D$  can  
298 amount to 0.1 or more, and dispersion should be taken  
299 into account (Lake, 1989; Bedrikovetsky, 1993). In a  
300 well neighbourhood, the reference radius of formation  
301 damage zone is 1 m, the heterogeneity reference size is  
302 also 1 m, so  $\varepsilon_D$  has order of magnitude of unity.

303 The dispersivity  $\alpha_D$  can reach several tens or even  
304 hundreds of meters at formation scales (Lake, 1989;  
305 Jensen et al., 1997); thus, the dimensionless dispersion  
306 can have the order of magnitude of unity, and hence  
307 hydrodynamic dispersion should be taken into account.

308 Now we formulate one dimensional problem for  
309 suspension injection into a porous core/reservoir.

310 The absence of suspended and retained particles in  
311 porous media before the injection is represented by the  
312 initial conditions:

$$t = 0 : c = \sigma = 0 \quad (12)$$

313 Fixing the inlet particle flux during the injection of  
316 particulate suspension in a reservoir determines the  
317 boundary condition:

$$x = 0 : Uc - D \frac{\partial c}{\partial x} = c^0 U \quad (13)$$

318 Sometimes the dispersive term in the boundary con-  
321 dition (Eq. (13)) is neglected (van Genuchten, 1981 and  
322 Nikolaevskij, 1990):

$$x = 0 : c = c^0 \quad (14) \quad 323$$



325 The particle motion in porous media can be decom-  
 326 posed into an advective flow with constant velocity and  
 327 the dispersive random walks around the front that  
 328 moves with advective velocity (Kampen, 1984). It is  
 329 assumed that once a particle leaves the core outlet by  
 330 advection it cannot come back by dispersion. This  
 331 assumption leads to the boundary condition of absence  
 332 of dispersion at the core outlet (Danckwerts, 1953;  
 333 Nikolaevskij, 1990):

$$x = L : \frac{\partial c}{\partial x} = 0 \quad (15)$$

336 In dimensionless coordinates (Eq. (A-1)), the pro-  
 337 posed model with a constant filtration coefficient takes  
 338 the form (Eqs. (A-10) and (11)):

$$\frac{\partial C}{\partial T} + v \frac{\partial C}{\partial X} = \varepsilon_D \frac{\partial^2 C}{\partial X^2} - \Lambda C \quad (16)$$

$$v = 1 - \Lambda \varepsilon_D \quad (17)$$

340 Neglecting the dispersion term in the capture kinet-  
 343 ics Eqs. (16) and (17) results in:

$$\frac{\partial C}{\partial T} + \frac{\partial C}{\partial X} = \varepsilon_D \frac{\partial^2 C}{\partial X^2} - \Lambda C \quad (18)$$

346 Eq. (18) is a traditional advective–diffusive model  
 347 with a sink term. The boundary condition (Eq. (13))  
 348 fixes the inlet flux in this model.

349 Eq. (16) looks like the advective–diffusive model  
 350 (Eq. (18)) with advective velocity  $v$ , and seems this  
 351 velocity should appear in the expression for the inlet  
 352 flux (Eq. (13)). However, the real advective velocity in  
 353 Eq. (16) is equal to one, and the delay term  $-\Lambda \varepsilon_D$   
 354 appears due to the capture of particles transported by  
 355 the dispersive flux and is not a part of the flux. From  
 356 conservation law (Eqs. (1) and (A-2)) it follows that the  
 357 particle flux is continuous at the inlet; the boundary  
 358 condition for Eq. (16) should be given by Eq. (13) that  
 359 differs from the inlet boundary condition for the equiv-  
 360 alent advective–diffusive model with the advective  
 361 velocity  $v$ .

362 Following Logan (2001), from now on the model  
 363 (Eq. (18)) will be referred to as the HLL model in order  
 364 to honour the fundamental work by Herzig et al.  
 365 (1970).

366 The difference between the presented and the HLL  
 367 model is the delay term  $\Lambda \varepsilon_D$  that appears in the advec-  
 368 tive flux velocity (Eq. (17)). This is the collective effect  
 369 of the particle dispersion and capture. Appearance of  
 370 the delay term  $\Lambda \varepsilon_D$  in the advective flux velocity (Eq.  
 371 (17)) is due to accounting for diffusive flux in the  
 372 capture kinetics (Eq. (2) and Eq. (4)).

A delay in the particle pulse arrival to the column  
 effluent if compared with the tracer pulse breakthrough  
 was observed by Massei et al. (2002).

The length  $L$  used in dimensionless parameters (Eq.  
 (A-1)) is a reference size of the boundary problem. It  
 affects the dimensionless filtration coefficient  $\Lambda$  (Eq.  
 (A-1)) and the inverse to Peclet number  $\varepsilon_D$ , (Eq. (11))  
 and drops out the delay term:  $\Lambda \varepsilon_D = \lambda \alpha_D$ . The dimen-  
 sionless time  $T$  corresponding to the length  $L$  (Eq. (A-  
 1)) is measured in “pore volume injected”, which is the  
 common unit in laboratory coreflooding and in field  
 data presentation.

Also, often the injected suspension is traced, and  
 the particle breakthrough curves are presented togeth-  
 er with tracer curves (Jin et al., 1997; Ginn, 2000). In  
 this case, the inverse to Peclet number  $\varepsilon_D$  in Eq. (16)  
 is already known from the tracer data and it is conve-  
 nient to use dimensionless variables and parameters  
 (Eq. (A-1)).

Nevertheless, Eq. (16) depends on two independent  
 dimensionless parameters —  $\varepsilon_D$  and  $\Lambda$ .

The inverse to filtration coefficient is an average  
 penetration depth of suspended particles (Herzig et  
 al., 1970), so the inverse to reference value of filtration  
 coefficient  $1/\lambda_0$  can be used as a reference length in  
 dimensionless linear co-ordinate (Eq. (A-12)). For  
 corresponding dimensionless variables (Eq. (A-12)),  
 the dimensionless  $\Lambda$  becomes equal to unit in the  
 case of constant filtration coefficient, and Eq. (16)  
 becomes dependent of one dimensionless parameter  $\varepsilon$   
 only, (Eq. (A-13)):

$$\frac{\partial C}{\partial T'} + v \frac{\partial C}{\partial X'} = \varepsilon \frac{\partial^2 C}{\partial X'^2} - C \quad (19)$$

$$v = 1 - \varepsilon, \quad \varepsilon = \lambda_0 \alpha_D$$

In the case of filtration function  $\Lambda = \Lambda(S)$ , Eq. (16)  
 includes deposited concentration  $S$ , and the model con-  
 sists of two equations

$$\begin{aligned} \frac{\partial C}{\partial T} + (1 - \Lambda(S) \varepsilon_D) \frac{\partial C}{\partial X} &= \varepsilon_D \frac{\partial^2 C}{\partial X^2} - \Lambda(S) C \\ \frac{\partial S}{\partial T} &= \Lambda(S) \left( 1 - \varepsilon_D \frac{\partial C}{\partial X} \right) \end{aligned} \quad (20)$$

for dimensionless parameters (Eq. (A-1)). 410

For dimensionless variables (Eq. (A-12)),  $\varepsilon_D$  must  
 be changed to  $\varepsilon = \lambda_0 \alpha_D$ . 412

The HLL in this case is also obtained by neglecting  
 dispersion term in capture rate expression. 414  
 415

416 The order of the governing system (Eq. (20)) can be  
417 reduced by one. Introducing the function

$$\Phi(S) = \int_0^S \frac{1}{\Lambda(s)} ds \quad (21)$$

418 from Eq. (A-3) we obtain:

$$\frac{\partial \Phi(S)}{\partial T} = Q \quad (22)$$

420 Substitution of Eq. (22) into Eq. (A-2) results in

$$\frac{\partial}{\partial T} (C + S) + \frac{\partial}{\partial X} \left( \frac{\partial \Phi(S)}{\partial T} \right) = 0 \quad (23)$$

423 Changing order of differentiation in the second term in  
426 the right hand side of Eq. (23) and integrating in  $T$  from  
427 zero to  $T$ , we obtain first order partial differential  
428 equation:

$$C + S + \frac{\partial \Phi(S)}{\partial X} = 0 \quad (24)$$

430 The integration constant that should appear in right  
432 hand side of Eq. (24) was calculated from initial con-  
433 ditions (Eq. (12)) — it is equal zero.

434 Eq. (22) becomes

$$\frac{\partial \Phi(S)}{\partial T} = 1 - \varepsilon_D \frac{\partial C}{\partial X} \quad (25)$$

435 Eqs. (24) and (25) form quasi-linear system of first  
438 order equations modeling deep bed filtration with size  
439 exclusion particle capture accounting for dispersion.

### 440 3. Dispersion free model

441 Neglecting the dispersion in Eq. (16) results in the  
442 simplified deep bed filtration model (Sharma and Yort-  
443 sos, 1987a,b,c; Elimelech et al., 1995; Tiab and  
444 Donaldson, 1996):

$$\frac{\partial C}{\partial T} + \frac{\partial C}{\partial X} = -\Lambda C \quad (26)$$

445 The boundary condition (Eq. (13)) automatically takes  
448 the form of Eq. (14).

449 The solution of the dispersion-free deep bed filtra-  
450 tion problem (Eqs. (26) (12) and (14)) is given by

$$C(X, T) = \begin{cases} \exp(-\Lambda X) & X \leq T \\ 0 & X > T \end{cases} \quad (27)$$

453 Concentration is zero ahead of the concentration front  
454  $X_0(T) = T$ . Particles arrive at the column outlet after one  
455 pore volume injection. Once the advancing front passes  
456 a given location, a steady concentration distribution is  
457 immediately established behind the front.

### 458 4. Transient flow in infinite reservoir

459 Let us consider flow in an infinite reservoir where,  
460 initially, water with particles fills the semi-infinite res-  
461 ervoir  $X < 0$ , and clean water fills the semi-infinite  
462 reservoir  $X > 0$ . Formula for concentration wave propa-  
463 gation (Eq. (B-2)) is presented in Appendix B.

464 Fig. 2 shows the concentration profiles for the times  
465  $T = 0.1, 1.0$  and  $4.0$  with  $\varepsilon_D = 1.0$  and  $\Lambda = 0.5$ . Solid  
466 lines correspond to the proposed model and dotted  
467 lines correspond to the HLL model. Both models ex-  
468 hibit advective propagation of the concentration wave  
469 with diffusive smoothing of the initial shock; the mix-  
470 ture zone expands with time. Suspended concentration  
471 is zero ahead of the mixture zone. Behind the mixture  
472 zone, concentration does not vary along the reservoir  
473 and exponentially decays with time due to deep bed  
474 filtration with a constant filtration coefficient. One can  
475 observe a delay in the concentration front propagation  
476 for the proposed model (Eq. (16)) if compared with the  
477 HLL model (Eq. (18)). The difference in the profiles in  
478 the two models appears in the mixture zone, while the  
479 concentrations ahead of and behind the mixture zone  
480 coincide for both models.

### 481 5. Analytical model for suspension injection into 482 semi-infinite reservoir

483 In this section we consider the particulate suspension  
484 injection into a semi-infinite reservoir,  $X > 0$ . The ex-  
485 pression for suspension concentration (Eq. (C-2)) is  
486 presented in Appendix C.

487 Fig. 3 depicts particle flux profiles for the dispersi-  
488 on. The concentration profiles at the moments  
489  $T = 0.5, 1.0, 2.0$  and  $6.0$  as obtained by explicit formula

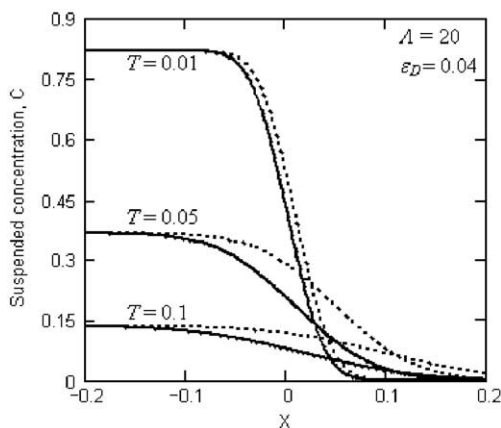


Fig. 2. Concentration wave dynamics in an infinite reservoir by the presented model and by the HLL model.

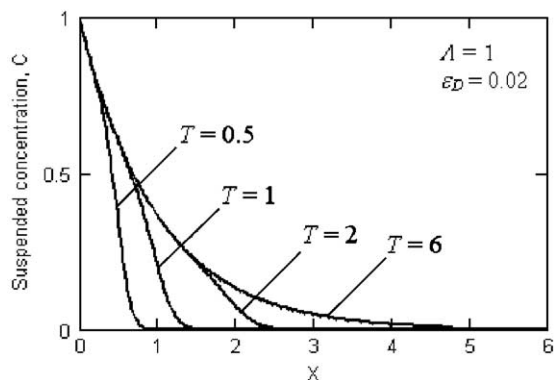


Fig. 3. Dynamics of concentration waves in a semi-infinite reservoir.

490 (Eq. (C-2)). The envelope curve corresponds to the  
 491 steady-state solution (Eq. (C-5)). Furthermore, for any  
 492 moment  $T$  there exists such position of a mixture zone  
 493  $X_0(T)$  that the transient and steady-state profiles behind  
 494 the zone ( $X < X_0(T)$ ) almost coincide. Once the transi-  
 495 tion zone passes a given location, the steady-state sus-  
 496 pended concentration distribution is established behind.  
 497 After establishing the steady state, all newly arrived  
 498 particles are captured by the rock, and the suspended  
 499 concentration is time-independent.

500 The term “steady state” is applied to the suspended  
 501 concentration only. The retained concentration  
 502 increases during the flow.

503 The particle flux profile in the steady-state regime  
 504 (Eq. (C-6)) shows that the  $\lambda$ th fraction of the particle  
 505 flux is captured under the steady-state conditions, and  
 506  $(1 - \lambda)$ th fraction passes through. The result must be  
 507 independent of the particle flux partition into the ad-  
 508 vective and dispersive parts, i.e. the formula for the  
 509 steady-state flux profile must not contain the dispersion  
 510 coefficient (Eq. (C-6)).

511 Fig. 4 depicts particle flux profiles for the disper-  
 512 sion-free model (solid line) and for the proposed model  
 513 using the solution (Eq. (C-5)) (dotted line) for  
 514  $\epsilon_D = 0.002$  and  $\Lambda = 1$ . The suspended concentration

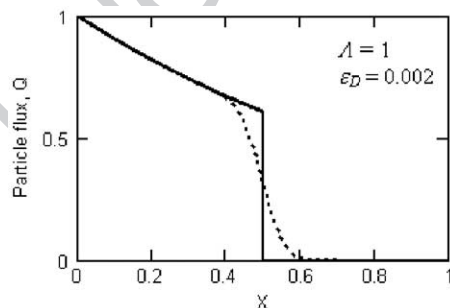


Fig. 4. Particle flux profile for  $T=0.5$  (semi-infinite reservoir) by the proposed model and the dispersion-free model.

515 and the particle flux coincide for dispersion-free flow,  
 516 and the profile is discontinuous. The introduction of  
 517 particle dispersion leads to smoothing the shock out.  
 518 The larger is the dispersion coefficient, the wider is the  
 519 smoothed zone around the shock.

520 Fig. 5 presents particle flux histories at the point  
 521  $X=1$  in a semi-infinite reservoir for the dispersion-free  
 522 case (curve  $\epsilon_D=0$ ) and three different dispersion values  
 523  $\epsilon_D=0.01, 0.1$  and  $0.5$ . On the one side, the higher is  
 524 the dispersion, the larger is the delay in the arrival of the  
 525 concentration front. On the other side, the larger is  
 526 the dispersion, the wider is the mixture zone about the  
 527 shock. Thus, the effect of the delay in advection com-  
 528 petes with that of the dispersion zone expansion. Fig. 5  
 529 shows fast breakthrough for large dispersion values.

530 Let us compare the stationary particle flux profiles  
 531 behind the moving mixture zone as obtained by the  
 532 proposed and HLL models. The solution can be  
 533 obtained from Eq. (C-2) by setting  $v=1$  and tending  
 534  $T$  to infinity. The calculation of the flux profile shows  
 535 that it is dispersion-dependent.

536 The asymptotic steady-state particle flux profile  
 537 (Eq. (C-6)) for the presented model coincides  
 538 with that for the dispersion-free model and is  
 539 dispersion-independent.

540 The comparative results are displayed in Fig. 6. The  
 541 flux is equal to 0.37 at  $X=1$  for both the proposed and  
 542 dispersion-free models. The HLL model profiles were  
 543 calculated for  $\epsilon_D=0.1, 1.0$  and  $3.0$ ; the corresponding  
 544 particle fluxes at  $X=1$  were found to be 0.40, 0.54 and  
 545 0.65, respectively.

546 The directions of diffusive and advective fluxes co-  
 547 incide. Therefore, inclusion of the diffusive flux into the  
 548 particle capture rate (Eq. (4)) increases the retention, and  
 549 the flux profile as calculated by the proposed model is  
 550 located below that as obtained by HLL model (Fig. 6).  
 551

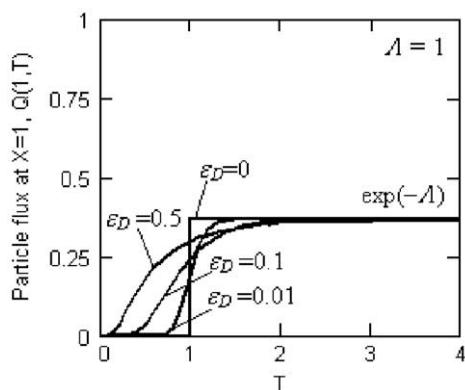


Fig. 5. Particle flux history at the point  $X=1$  in semi-infinite reservoir for different dispersion coefficients.

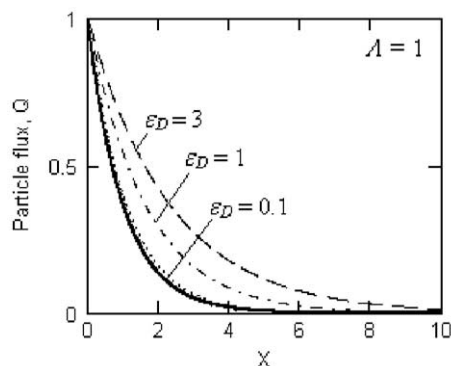


Fig. 6. Steady-state particle flux profiles for the dispersion-free case and by the presented model (the same solid curve) and by the HLL model with  $\varepsilon_D=0.1$ ,  $\varepsilon_D=1.0$  and  $\varepsilon_D=3$  (dotted, dot-and-dash and dashed lines, respectively).

551 One may notice a significant difference between the  
 552 two profiles as calculated by the proposed and the HLL  
 553 model for large dimensionless dispersion ( $\varepsilon_D=1.0$  and  
 554 3.0); the difference is negligible for  $\varepsilon_D$  less than 0.1.  
 555 The dependence of the particle flux at  $X=1$  on the  
 556 dimensionless dispersion  $\varepsilon_D$  is plotted in Fig. 7 for  
 557 the proposed model (solid line) and the HLL model  
 558 (dashed line). As mentioned before, the particle flux  
 559 predicted by the proposed model is independent of  
 560 dispersion for the steady-state regime (Eq. (C-6)),  
 561 which implies that the solid line is horizontal.

562 Consider the asymptotic case where the Peclet num-  
 563 ber vanishes. As  $\varepsilon_D \gg 1$ , the flux in the HLL model  
 564 tends to unity; hence the steady-state flux is constant  
 565 along the column and no particle is captured, which is  
 566 unphysical. For large dispersion, the advective flux is  
 567 relatively low; the capture rate in the HLL model is  
 568 proportional to the advective flux and, therefore, is also

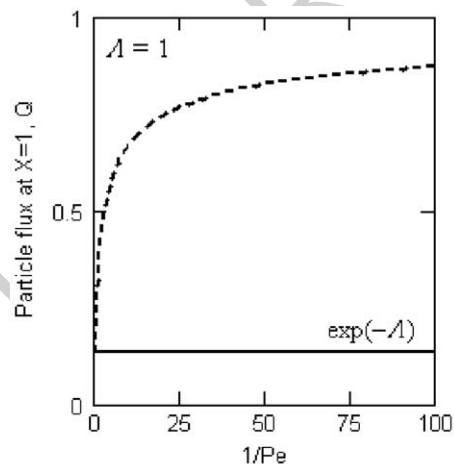


Fig. 7. Effect of dispersion on the flux at  $X=1$  for the steady-state mode in a semi-infinite reservoir for proposed and HLL models.

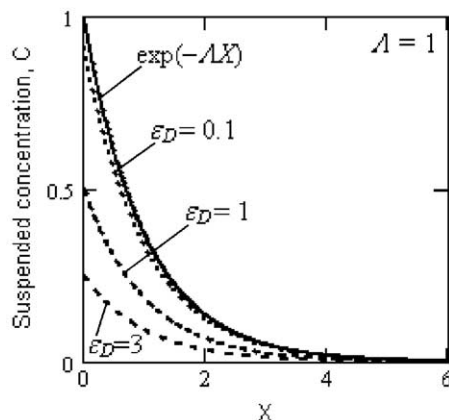


Fig. 8. Comparison between steady-state concentration profiles for deep bed filtration in a semi-infinite reservoir taking into account and neglecting dispersion in the inlet boundary conditions.

low. Thus, particle capture vanishes as  $\varepsilon_D \gg 1$ . No  
 569 particle retention occurs when the dispersive mass  
 570 transfer dominates over the advection.  
 571

The obtained contradiction occurs because the HLL  
 572 model does not account for capture of particles trans-  
 573 ported by dispersive flux (Fig. 8).  
 574

## 6. Filtration in semi-infinite reservoir with simplified inlet boundary conditions

Let us discuss the case where dispersion is neglected  
 577 in the inlet boundary condition (Eq. (14)). The exact  
 578 solution is obtained in Appendix D, (Eq. (D-1)).  
 579

The concentration profile in steady-state regime (Eq.  
 580 (D-2)) coincides with the concentration profile for the  
 581 dispersion-free model. The simplified inlet boundary  
 582 condition (Eq. (14)) is the same as the one for the  
 583 dispersion-free model. Hence, the introduction of dis-  
 584 persion into the deep bed filtration model while keeping  
 585 the same boundary condition (Eq. (14)) does not change  
 586 the asymptotic profile of the suspended concentration.  
 587

Fig. 6 shows steady-state concentration profiles for  
 588 the simplified inlet boundary condition, given by Eq.  
 589 (D-2) (solid line) and for the complete inlet boundary  
 590 condition, given by Eq. (C-5) (dotted curves). Three  
 591 dotted curves correspond to  $\varepsilon_D=0.1$ , 1.0 and 3.0. The  
 592 inlet concentration for dotted lines is always less than  
 593 unity. The higher is the dispersion the lower is the  
 594 stationary concentration under the fixed inlet flux.  
 595

## 7. Steady-state solution for filtration in finite cores

The expression for the particle flux profile in steady-  
 597 state regime (Eq. (E-2)) coincides with the flux profile  
 598 behind the mixture zone in semi-infinite media. The  
 599



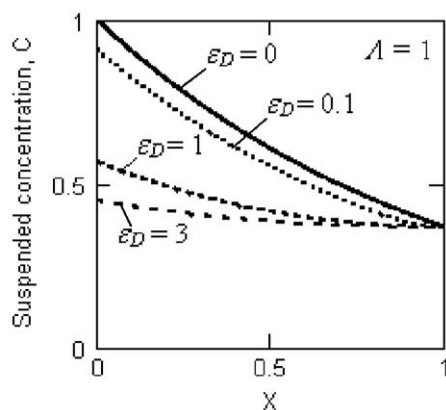


Fig. 9. Steady-state suspended concentration profiles for filtration in a limited core for  $\varepsilon_D=0, 0.1, 1.0$  and  $3.0$  (solid, dotted, dashed and dot-and-dash lines, respectively).

concentration profiles are different because the boundary condition of the dispersion absence is set at the core outlet  $X=1$  for the finite cores and at  $X \rightarrow \infty$  for semi-infinite media.

The inlet concentration (Eq. (E-4)) is less than unity. It decreases as dispersion increases. By letting  $\varepsilon_D \rightarrow \infty$  in Eq. (E-4), we find that the inlet concentration tends to  $\exp(-\lambda)$ , which is the outlet concentration (Eq. (E-5)). Hence, as dispersion tends to infinity, the suspended concentration profile becomes uniform.

Fig. 9 shows suspended concentration profiles for  $\varepsilon_D=0.1, 1.0$  and  $3.0$ . The inlet concentration for  $\varepsilon_D=0.1$  is equal to  $0.91$ . For  $\varepsilon_D=3.0$  the profile is almost uniform.

It is important to emphasize that the outlet concentration (Eq. (E-5)) is independent of the dispersion coefficient and is determined by the filtration coefficient only. This fact is in agreement with the presented above interpretation of the filtration coefficient:  $\lambda$  is the probability for a particle to be captured by the sieve. The outlet concentration coincides with the particle flux due to the outlet boundary condition (Eq. (A-7)). Therefore, the outlet concentration under the steady-state conditions must be determined by the probability for a particle to be captured and must be independent of dispersion. The outlet concentration predicted by the HLL model depends on the dispersion coefficient.

It is worth mentioning that the retention profile (Eq. (E-6)) is dispersion independent. This is because the capture rate is proportional to the total particle flux (Eq. (E-2)).

## 8. Treatment of laboratory data

The formula for steady state limit of the outlet concentration (Eq. (E-5)) allows determining the filtra-

tion coefficient from the asymptotic value of the breakthrough curve. From Eq. (E-5) it follows that

$$\lambda = -\ln C(1) \quad (28)$$

Formula Eq. (28) coincides with that for determining the filtration coefficient from the asymptotic value of the breakthrough curve using the dispersion-free model (Eq. (26)), see (Pang and Sharma, 1994). The dispersion acts only in the concentration front neighbourhood, the asymptotic value for the breakthrough concentration is dispersion-independent.

Let us find out which model provides better fit to the experimental data. First, we determine the intervals for the test parameters where the difference between the modelling data by the two models is significant.

The proposed and HLL models differ by the delay term  $\lambda \varepsilon_D$  in the advective velocity. The models coincide as  $\varepsilon_D=0$ . Hence, the larger is the dispersivity, the higher should be the difference between the two models.

Fig. 10 shows the core outlet flux for the steady-state regime with different  $\lambda$  and  $\varepsilon_D$  as calculated by the proposed model (solid line) and the HLL model (dashed line). The marked points on dashed curves correspond to the value of  $\varepsilon_D$  where the difference between the proposed and HLL models starts to exceed 10%. For  $\lambda=4, 1$  and  $0.55$ , the 10%, the difference between the outlet fluxes can be observed for  $\varepsilon_D$  greater than  $0.006, 0.13$  and  $1.74$ , respectively. The value  $\lambda=4$  is typical for seawater injected in medium permeability cores. The value  $\lambda=0.55$  is typical for virus transport in highly permeable porous columns. The typical core size  $L=0.1$  m. So, in order to validate the proposed and HLL models, one should perform laboratory coreflood with seawater in cores with dispersivity exceeding

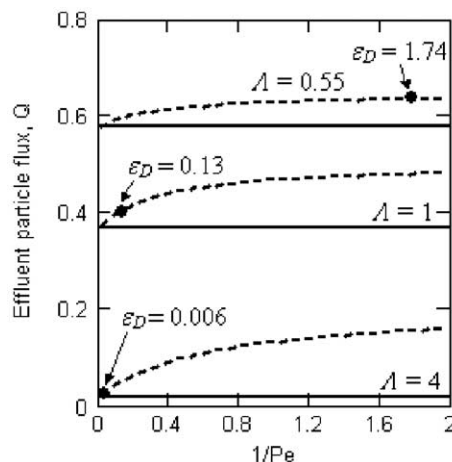


Fig. 10. Effect of dispersion on the particle flux at the core outlet for steady-state flows.

685  $10^{-3}$  m; the core dispersivity for virus transport should  
 686 exceed 0.2 m.

687 In papers by Ginn, 2000 and Jin et al., 1997, the  
 688 outlet concentrations during the injection of particulate  
 689 suspensions into sand porous columns were measured  
 690 in laboratory tests. Flow experiments on the transport of  
 691 oocysts bacteria and pathogenic viruses were carried  
 692 out in these studies. Laboratory test parameters are  
 693 presented in Table 1, where the first and the second  
 694 lines correspond to tests presented in Ginn, 2000, four  
 695 other tests are taken from the paper by Jin et al., 1997.  
 696 The breakthrough curves in Fig. 11a, b correspond to  
 697 tests 2 and 3. The filtration coefficients are calculated  
 698 from the asymptotic values  $C(X=1, T \rightarrow \infty)$  by Eq.  
 699 (28) and are presented in Table 2.

700 In the laboratory tests in both works, the injected  
 701 water was traced, and the tracer outlet concentrations  
 702 were measured. Chloride and bromide tracers were used  
 703 in order to determine the dispersion coefficient. The  
 704 particle dispersion was assumed to be equal to the tracer  
 705 dispersion. The values of dispersion coefficient are  
 706 given in Table 1. Comparing the  $\epsilon_D$  values in Fig. 10  
 707 and those in Table 1, one could conclude that there  
 708 should be no significant difference between the proposed  
 709 and HLL models for low values of dispersion in  
 710 the laboratory tests.

711 Matching the laboratory data in limited cores by the  
 712 analytical model for flow in a semi-infinite reservoir  
 713 was suggested by Unice and Logan (2000). Fig. 11a  
 714 and b depict breakthrough curves calculated by the  
 715 analytical model (Eq. (C-2)) using the values of  $\lambda$   
 716 and  $\epsilon_D$  from Tables 1 and 2.

717 From Fig. 11a and b it is apparent that both models  
 718 describe the experimental data equally well.

719 The difference between the filtration coefficients as  
 720 predicted by the different models (second and third  
 721 columns of the table) is not very high due to low  
 722 dispersion of the porous media used in laboratory  
 723 tests. A typical value of the filtration coefficient in  
 724 Table 2 is  $\lambda=1.4$ , and hence the two models would

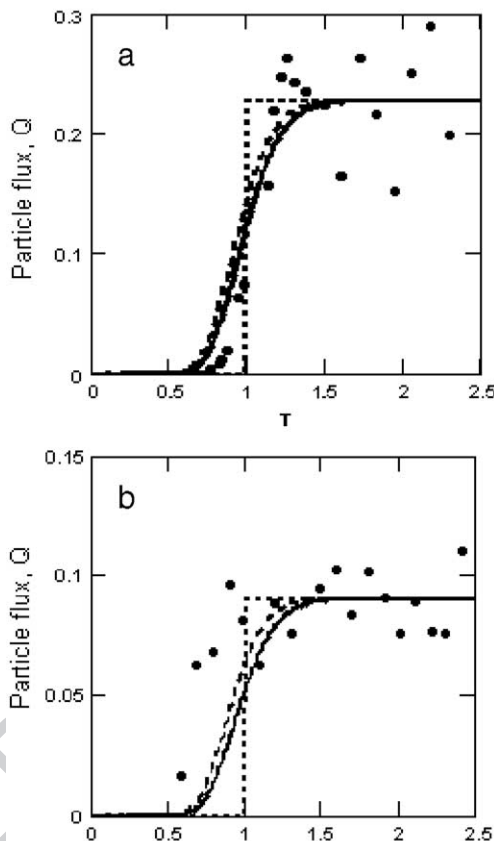


Fig. 11. Matching the breakthrough curves by the proposed and the HLL models (solid and dashed lines, respectively).

725 give different results for  $\epsilon_D$  greater higher 0.15. The  
 726 Table 1 shows that typical values of  $\epsilon_D$  for tests 3–6 are  
 727 0.02, and hence a noticeable difference between the two  
 728 models cannot be anticipated.

729 The proposed model assumes that the capture rate is  
 730 proportional to the total flux, while the HLL model  
 731 assumes that the capture rate is proportional to the  
 732 advective flux only. Consequently, the flux in the cap-  
 733 ture kinetics of the HLL model is lower than that of the  
 734 presented model. Therefore, the filtration coefficient  
 735 should be higher in the HLL model rather than in the  
 736 proposed model in order to fit the same retaining ki-  
 737 netics value.

738 The comparison between the second and the third  
 739 columns of Table 1 shows that the filtration coefficient  
 740 predicted by the HLL model is higher than that pre-  
 741 dicted by the proposed model which confirms the above  
 742 presented speculations.

743 However, due to low dispersion in laboratory tests,  
 744 the difference in the values of the filtration coefficient  
 745 values from the two models is not sufficiently high for  
 746 validation of the proposed and HLL models.

t1.1 Table 1  
 Summary of experiments by Ginn (2002) and Jin et al. (1997)

t1.3	Test no	Column length $L$ (cm)	Flow rate $J_w$ (cm/h)	Dispersion coeff. $D$ (cm <sup>2</sup> /h)	Dispersivity $\alpha_D$ (cm)	Dimensionless dispersion $\epsilon_D$
t1.4	Exp.1	10.0	29.6	7.70	0.26	0.026
t1.5	Exp.2	10.0	2.96	0.53	0.18	0.018
t1.6	Exp.3	20.0	3.35	1.23	0.37	0.02
t1.7	Exp.4	20.0	3.19	1.13	0.35	0.02
t1.8	Exp.5	20.0	3.11	1.13	0.36	0.02
t1.9	Exp.6	10.5	2.99	0.76	0.25	0.02

t2.1 Table 2  
 t2.2 Filtration coefficient as obtained from breakthrough curves by the proposed and the HLL models

t2.3 Test no	$\lambda$ by proposed model and by dispersion free model	$\lambda$ by HLL model
t2.4 Exp.1	0.59	0.6
t2.5 Exp.2	2.40	2.51
t2.6 Exp.3	1.48	1.52
t2.7 Exp.4	1.56	1.60
t2.8 Exp.5	1.38	1.42
t2.9 12/exp.6	0.75	0.76

747 The proposed and dispersion-free models give the  
 748 same filtration coefficient value, because they use the  
 749 same equation for the inverse problem (Eq. (28)).  
 750 For large  $\epsilon_D$ , the values of  $\lambda$  calculated by the two  
 751 models would differ significantly. For example, for  
 752  $\epsilon_D=1$  and asymptotic outlet concentration  $C=0.06$ ,  
 753 the filtration coefficients predicted by the proposed  
 754 and the HLL models are 2.8 and 7.1, respectively. The  
 755 data from natural reservoir cores rather than that from  
 756 sand columns may be used for validation of the model.

9. Travelling dispersion wave

758 Let us find the travelling wave solution for system  
 759 (Eq. (20)) with dynamic blocking filtration coefficient  
 760 (Eq. (5)):

$$C = C(w), S = S(w), w = X - uT \tag{29}$$

762 where  $u$  is the unknown wave speed.  
 763 The travelling wave solution of the deep bed filtra-  
 764 tion system (Eq. (20)) is described by non-linear dy-  
 765 namic system (Eq. (F-7)) in plane  $(C, S)$ . The phase  
 766 portrait is shown in Fig. 12. The analysis of the dy-  
 767 namic system is analogous to that performed by D.  
 768 Logan (2001), for HLL model.  
 769 The system has two singular points. The point  $(0, 0)$   
 770 correspond to the initial conditions (Eq. (12)), i.e. to the

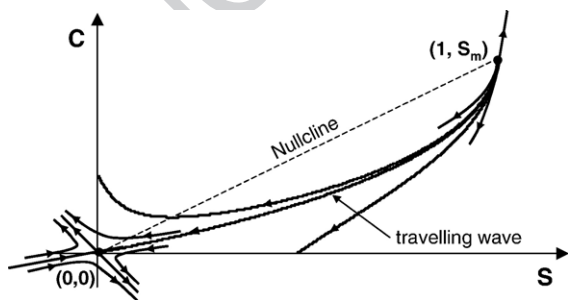


Fig. 12. Phase portrait of the dynamic system for dynamic blocking function.

771 absence of particles before the injection, and point  $(1, S_m)$ ,  
 772 corresponds to the boundary condition (Eq. (14)),  
 773 i.e. to the final equilibrium state  $(1, S_m)$ , where  $S_m$  is the  
 774 maximum number of retained particles per unit of rock  
 775 volume. Point  $(0, 0)$  is a saddle point, the two orbits  
 776 leaving the origin are unstable manifolds, and the two  
 777 orbits entering the origin are stable manifolds. Point  $(1, S_m)$   
 778 is an unstable repulsive node.

779 As shown in Fig. 12, there is only one trajectory that  
 780 links the two singular points, and this trajectory is the  
 781 travelling wave solution. The travelling wave joins  
 782 initial and final equilibrium states of a system.

783 The travelling wave speed (Eq. (F-6)) was calculated  
 784 in Appendix F:

$$0 < u = \frac{1}{1 + S_m} < 1 \tag{30}$$

785 At large length scale exceeding the travelling wave  
 786 thickness, the wave (Eq. (29)) degenerates into shock  
 787 wave. The speed (Eq. (30)) fulfils the Hugoniot condi-  
 788 tion of mass balance on the shock that corresponds to  
 789 conservation law (Eq. (1)) (Bedrikovetsky, 1993).  
 790 Therefore, the speed (Eq. (30)) for the proposed system  
 791 (Eq. (20)) is the same as that for HLL model (Logan,  
 792 2001), since conservation law (Eq. (1)) is the same for  
 793 either model.

794 The solution of initial-boundary value problem (Eqs.  
 795 (12) and (14)) asymptotically tends to travelling wave  
 796 for the case of blocking filtration function, (Eq. (5)).  
 797 The travelling wave solution is invariant with respect to  
 798 a shift along the axes  $x$ . The shift can be fixed at any  
 799 time in order to provide an approximate solution for the  
 800 initial-boundary value problem (Tikhonov and Samars-  
 801 802

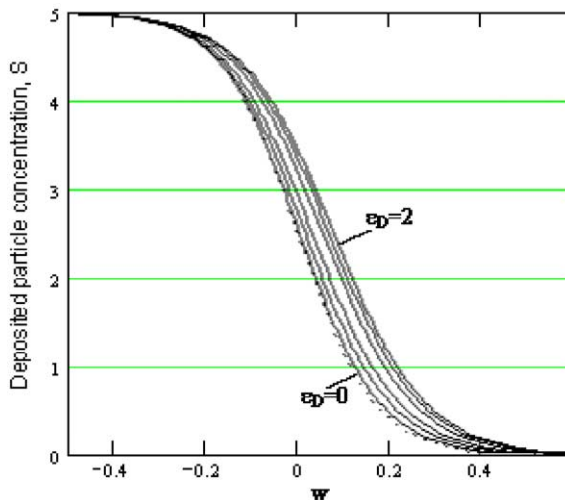


Fig. 13. Travelling wave solution without dispersion (traced line) and with dispersion (solid lines), for  $D = 0.03, 0.1, 0.2, 0.5, 1$  and  $2$ .

803 kii, 1990). Calculations in Appendix F show that the  
804 travelling wave fulfils the total mass balance for sus-  
805 pended and retained particles (Eq. (1)) if and only if it  
806 obeys the Goursat condition at the inlet  $x=0$ . It allows  
807 choosing the shift at any time  $T$  that the total mass  
808 balance is fulfilled, see Eqs. (F-14) and (15).

809 The retained concentration profiles are shown in Fig.  
810 13 for several dispersion coefficients. The following  
811 data were used: linear blocking function (Eq. (6))  
812  $\Lambda(S)=10-2S$ ,  $c_0=100$  ppm and  $\phi=0.2$ . The disper-  
813 sive wave ( $\varepsilon_D>0$ ) travels ahead of the dispersion-free  
814 wave, and the wave velocities are equal. The higher is  
815 the dispersion coefficient the more advanced is the  
816 travelling wave.

### 817 10. Three dimensional deep bed filtration with 818 dispersion

819 Let us derive three dimensional deep bed filtration of  
820 multi component suspension in porous media with size  
821 exclusion mechanism of particle capture on the macro  
822 scale. Particle populations with densities  $\rho_i$ ,  $i=1,2..n$ ,  
823 flow in porous rock with velocities  $U_i$ .

824 Particle capture in one dimension is modelled in  
825 Section 2 by a sieve sequence. The filtration coefficient  
826  $\lambda_i$  for each population is defined as a fraction of parti-  
827 cles captured per unit of the particle trajectory. We  
828 introduce the reference distance  $l$  between the sieve  
829 surfaces. Generally speaking,  $l$  is a continuous function  
830 of  $(x, y, z)$ , where  $(x, y, z)$  is a point of three dimen-  
831 sional flow domain. A sieve captures  $\lambda_i l$ -th fraction of  
832 passing particles of  $i$ -th population, i.e. if  $\rho_i U_i$  is a flux  
833 of  $i$ -th population particles entering the “core” which is  
834 perpendicular to the sieves, the particle capture rate is  
835  $\lambda_i l \rho_i U_i$ , (Fig. 1).

836 The sieve surface has locally a plane form, so the  
837 sieves filling the three dimensional domain form two-  
838 dimensional vector bundle. Existence of a reference  
839 distance  $l$  between the sieve surfaces is consistent  
840 with the assumption of integrability of the vector bun-  
841 dle. Therefore, we consider the foliation case where the  
842 sieves are located on the surfaces where a smooth  
843 function  $f(x, y, z)$  is constant.

844 For  $i$ -th population flux, the particle capture rate in a  
845 reference volume  $V$  is proportional to the flux projec-  
846 tion on the vector perpendicular to the sieve. So, one-  
847 dimensional product  $\lambda_i l \rho_i U_i$  (Eq. (4)) is substituted by  
848 the scalar product of the flux vector and the unit length  
849 vector perpendicular to the sieve:

$$850 \lambda_i \left\langle \frac{\nabla f}{|\nabla f|}, \rho_i U_i \right\rangle V \quad (31)$$

Therefore, the particle mass balance for  $i$ -th 852  
population with the consumption rate (Eq. (31)) 853  
becomes: 854

$$\frac{\partial \rho_i}{\partial t} + \text{div}(\rho_i U_i) = -\lambda_i \left\langle \frac{\nabla f}{|\nabla f|}, \rho_i U_i \right\rangle \quad (32)$$

Introduce average mass density and velocity of the 855  
overall multi component flux 858

$$\rho = \sum_i \rho_i, U = \sum_i \frac{\rho_i U_i}{\rho} \quad (33)$$

The diffusive flux of  $i$ -th component around the 860  
front moving with the average velocity  $U$  is defined 862  
as a difference between the  $i$ -th component flux moving 863  
with the  $i$ -th component velocity and that with the 864  
average velocity (Landau and Lifshitz, 1987; Niko- 865  
laevskij, 1990) 866

$$\rho_i U_i = c_i \rho U - D_i \rho \nabla c_i \quad (34)$$

Assuming incompressibility of the mixture 869

$$\rho = \text{const}, \text{div} U = 0 \quad (35)$$

and substituting Eqs. (34) and (35) into Eq. (32), we 870  
obtain the following form of the particle mass balance 872  
for  $i$ -th population accounting for particle dispersion 873  
and capture 874

$$\frac{\partial c_i}{\partial t} + \langle U, \nabla c_i \rangle = D_i \Delta c_i - \lambda_i \left\langle \frac{\nabla f}{|\nabla f|}, c_i U - D_i \nabla c_i \right\rangle \quad (36)$$

Opening brackets of the scalar product in right hand 875  
side of Eq. (36) and grouping terms in the left and right 878  
hand sides, we obtain 879

$$\frac{\partial c_i}{\partial t} + \left\langle U - \lambda_i D_i \frac{\nabla f}{|\nabla f|}, \nabla c_i \right\rangle = D_i \Delta c_i - \lambda_i \left\langle \frac{\nabla f}{|\nabla f|}, U \right\rangle c_i \quad (37)$$

Eq. (37) is a three dimensional generalization of Eq. 880  
(16). It allows describing the anisotropy capture effect 883  
where the filtration coefficient depends on the flow 884  
direction, while three dimensional generalization of 885  
HLL Eq. (18) can describe just a scalar (isotropic) 886  
particle capture. 887

The first term in the scalar product in the left hand 888  
side of Eq. (37) consists of the average flow velocity  $U$  889  
and the velocity with module  $\lambda_i D_i$  directed perpendic- 890  
ular to sieve surfaces. So, the collective effect of disper- 891  
sion with capture results in slowing down the 892  
advective particle flux. 893



894 **11. Summary and conclusions**

895 The particle size exclusion capture rate in deep bed  
896 filtration is proportional to the total particle flux includ-  
897 ing both the advective and the dispersive flux compo-  
898 nents. Therefore, the dispersion term must be present  
899 not only in the particle balance equation but also in the  
900 capture kinetics equation.

901 The outlet concentration for steady-state flow in a  
902 limited core is completely determined by the particle  
903 capture probability; therefore, it is independent of the  
904 dispersion coefficient. The outlet concentration by the  
905 model proposed is independent of dispersion, while  
906 that by the traditional HLL model is dispersion  
907 dependent.

908 The steady state flux profile in semi-infinite and  
909 limited size porous media should be also dispersion-  
910 independent, as the proposed model shows. The HLL  
911 model exhibits dependency of steady state flux profile  
912 on dispersion.

913 It allows concluding that for steady state flows the  
914 proposed model exhibits physically coherent results,  
915 while the traditional model exhibits physically unreal-  
916 istic behaviour.

917 The collective effect of dispersion and capture on  
918 deep bed filtration in the model proposed is a delay  
919 in the propagation of the advective concentration  
920 wave.

921 A constant filtration coefficient can be determined  
922 from the asymptotical steady-state outlet concentration  
923 during a transient coreflood test using the proposed  
924 model without knowing the dispersion coefficient,  
925 while the dispersion coefficient should be known in  
926 order to calculate the filtration coefficient by the HLL  
927 model.

928 The constant filtration coefficient as determined  
929 from the asymptotical value of effluent concentration  
930 using the proposed model is equal to that determined by  
931 the dispersion-free model. Therefore, the HLL and the  
932 proposed models show equally satisfactory fit with the  
933 data of available experiments under small dispersivity.

934 Laboratory experiments in heterogeneous cores with  
935 high dispersivity should be carried out in order to  
936 validate the proposed model.

937 The travelling wave regime of deep bed filtration  
938 with dispersion exists for the blocking type of filtra-  
939 tion coefficient only. The velocity of the travelling  
940 wave is determined by the maximum concentration  
941 of retained particles and is independent of dispersion  
942 coefficient. The higher is the maximum retained par-  
943 ticle concentration the lower is the travelling wave  
944 speed.

The proposed three dimensional model allows de- 945  
scribing anisotropic particle capture while 3D HLL 946  
model describes only scalar (isotropic) capture of sus- 947  
pended particles. 948

**12. Uncited reference** 949

Harter et al., 2000 950

*Nomenclature* 952

$c$	Suspended particles concentration	953
$c^0$	Inlet suspended particles concentration	954
$C$	Dimensionless suspended particle concentration	955
$D$	Dispersion coefficient	956
$k^0$	Original permeability	957
$l$	Distance between sieves	958
$p$	Pressure	959
$P$	Dimensionless pressure	960
$q$	Particle flux	961
$Q$	Dimensionless particle flux	962
$s$	Laplace coordinate	963
$S$	Dimensionless retained particles concentration	964
$t$	Time	965
$T$	Dimensionless time	966
$U$	Darcy's velocity	967
$v$	Delay term in the advective velocity	968
$x$	Linear co-ordinate	969
$X$	Dimensionless co-ordinate	970
$w$	Transformation variable	971
$\alpha_D$	Dispersivity	972
$\beta$	Formation damage coefficient	973
$\varepsilon_D$	Dimensionless dispersion coefficient	974
$\phi$	porosity	975
$\lambda$	Filtration coefficient	976
$\Lambda$	Dimensionless filtration coefficient	977
$\mu$	Suspension viscosity	978
$\sigma$	Retained particle concentration	979

**Acknowledgements** 981

The authors are grateful to Profs. Yannis Yortsos 982  
(South California University, USA), Oleg Dinariev 983  
(Institute of Earth Physics, Russian Academy of 984  
Sciences), Dan Marchesin (Institute of Pure and Ap- 985  
plied Mathematics, Brazil) and Mikhael Panfilov 986  
(ENSG — INPL, Nancy, France) for the fruitful dis- 987  
cussions. The collaboration with Adriano Santos 988  
(North Fluminense State University, UENF/Lenep, 989  
Brazil) is highly acknowledged. 990

Special thanks are due to Prof. Themis Carageorgos 991  
(UENF/Lenep) for support and encouragement. 992

993 **Appendix A. Dimensionless governing equations**

994 Introduction of dimensionless variables and  
995 parameters

$$X = \frac{x}{L}, T = \frac{Ut}{\phi L}, C = \frac{c}{c^0}, S = \frac{\sigma}{c^0 \phi}, A(S) = \lambda(\sigma)L,$$

$$P = \frac{k_0 p}{U \mu L}, Q = \frac{q}{c^0 U}, \varepsilon_D = \frac{\alpha_D}{L} \quad (A-1)$$

996 transforms the governing Eqs. (1) (2) (4) and (9)  
998 to the following form:

$$\frac{\partial}{\partial T}(C + S) + \frac{\partial Q}{\partial X} = 0 \quad (A-2)$$

999  $\frac{\partial S}{\partial T} = A Q \quad (A-3)$

1000  $Q = C - \varepsilon_D \frac{\partial C}{\partial X} \quad (A-4)$

1001  $-\frac{1}{(1 + \beta \phi c^0 S)} \frac{\partial P}{\partial X} = 1 \quad (A-5)$

1002 The boundary conditions (Eqs. (13) and (15)) in  
1005 dimensionless variables (Eq. (A-1)) take the form:

$$X = 0 : Q = C - \varepsilon_D \frac{\partial C}{\partial X} = 1 \quad (A-6)$$

1006  $X = 1 : \frac{\partial C}{\partial X} = 0 \quad (A-7)$

1008 The simplified boundary condition (Eq. (14)) becomes:

$$X = 0 : C = 1 \quad (A-8)$$

1010 The initial conditions (Eq. (12)) remain the same.

1013 Substituting the capture rate expression (Eq. (A-3))  
1014 into the mass balance Eq. (A-2), we obtain:

$$\frac{\partial C}{\partial T} + \frac{\partial Q}{\partial X} = -A Q \quad (A-9)$$

1015 Substituting Eq. (A-4) into Eq. (A-9) yields the follow-  
1018 ing parabolic equation:

$$\frac{\partial C}{\partial T} + v \frac{\partial C}{\partial X} = \varepsilon_D \frac{\partial^2 C}{\partial X^2} - A C \quad (A-10)$$

1019  $v = 1 - A \varepsilon_D \quad (A-11)$

1020 Introduction of other dimensionless time, linear co-  
1023 ordinate, pressure and filtration coefficient

$$X' = \lambda_0 x, T' = \frac{U \lambda_0 t}{\phi}, A'(S) = \frac{\lambda(\sigma)}{\lambda_0}, P' = \frac{k_0 p \lambda_0}{U \mu} \quad (A-12)$$

keeps Eqs. (A-2) (A-3) and (A-5) the same; Eq. (A-4) becomes

$$Q = C - \varepsilon \frac{\partial C}{\partial X'}, \varepsilon = \alpha_D \lambda_0 \quad (A-13)$$

**Appendix B. Flow in an infinite reservoir**

Let us consider flow in an infinite reservoir where, initially, water with particles was filling the semi-infinite reservoir  $X < 0$ , and clean water was filling the semi-infinite reservoir  $X > 0$  (so-called Riemann problem):

$$T = 0 : C(X, 0) = \begin{cases} 1, X < 0 \\ 0, X > 0 \end{cases} \quad (B-1)$$

Boundary conditions  $C=0$  and  $C=1$  must be satisfied at  $X \rightarrow \infty$  and  $X \rightarrow -\infty$ , respectively.

The filtration coefficient is supposed to be constant.

The solution for deep bed filtration in an infinite reservoir Eqs. (A-10) and (B-1) can be obtained in explicit form (Polyanin, 2002):

$$C(X, T) = \frac{1}{2} \left[ \exp(-AT) \operatorname{erfc} \left( \frac{X - vT}{2\sqrt{\varepsilon_D T}} \right) \right] \quad (B-2)$$

**Appendix C. Transient solution for a semi-infinite reservoir**

Let us discuss the particulate suspension injection into a semi-infinite reservoir,  $X > 0$ . The initial and boundary conditions are defined by Eqs. (12) (A-6) (A-7), respectively. The condition  $C=0$  for a semi-infinite reservoir should be satisfied at  $X \rightarrow \infty$ .

The explicit solution of the problem is obtained by substitution

$$C(X, T) = \exp(-AT) w(X, T) \quad (C-1)$$

and by Laplace transform in  $T$  (Polyanin, 2002):

$$C(X, T) = \frac{1}{A} \exp \left[ \frac{(v-A)X}{2\varepsilon_D} \right] \operatorname{erfc} \left( \frac{X-AT}{B} \right) - \frac{1}{A} \exp \left[ \frac{(v+A)X}{2\varepsilon_D} \right] \operatorname{erfc} \left( \frac{X+AT}{B} \right) - \frac{(2-v)}{2\varepsilon_D} \exp \left( \frac{X}{\varepsilon_D} \right) \times \int_0^T \operatorname{erfc} \left( \frac{X+(2-v)t}{2\sqrt{\varepsilon_D t}} \right) dt \quad (C-2)$$

$$A = \sqrt{v^2 + 4A\varepsilon_D} \quad (C-3)$$

$$B = 2\sqrt{\varepsilon_D T} \quad (C-4)$$

1024  
1026

1028  
1029

1030  
1031  
1032  
1033

1036  
1037

1038

1039

1040

1041

1042

1044

1045

1046

1047

1048

1049

1050

1051

1052

1053

1055

1056

1058 The solution (Eq. (C-2)) reaches steady state as  $T \rightarrow \infty$ :

$$C(X, \infty) = \frac{1}{1 + A\varepsilon_D} \exp(-AX) \quad (C-5)$$

1060 Formula Eq. (C-5) is a steady-state solution of the  
1062 boundary-value problem (x) and (x).

1063 Eq. (C-5) allows calculation of the particle flux  
1064 profile in the steady-state regime:

$$Q(X) = \exp(-AX) \quad (C-6)$$

1066

1067 **Appendix D. Filtration in semi-infinite reservoir**  
1068 **with simplified inlet boundary conditions**

1069 Let us discuss the simplified case where dispersion  
1070 is neglected in the inlet boundary conditions. Eq. (A-  
1071 10) is subject to initial condition Eq. (12), inlet bound-  
1072 ary condition (Eq. (A-8)/Eq. (14)); the condition  $C=0$   
1073 must be satisfied as  $X \rightarrow \infty$ .

1074 The problem is solved using the Laplace transform  
1075 in  $T$  (Polyanin, 2002):

$$C(X, T) = \frac{1}{2} \left[ \exp\left(\frac{X}{\varepsilon_D}\right) \operatorname{erfc}\left(\frac{X + MT}{B}\right) + \exp(-AX) \operatorname{erfc}\left(\frac{X - MT}{B}\right) \right] \quad (D-1)$$

1076  $M = 1 + A\varepsilon_D$

1078 where constant  $B$  is given by formula Eq. (C-16).

1079 The solution (Eq. (D-1)) tends to steady-state as-  
1080 ymptotic as  $T \rightarrow \infty$ :

$$C(X, \infty) = \exp(-AX) \quad (D-2)$$

1082

1083 **Appendix E. Steady-state solution for filtration in**  
1084 **finite cores**

1085 The equation for steady state in finite cores corre-  
1086 sponds to zero time derivative in Eq. (A-9):

$$\frac{dQ}{dX} = -AQ \quad (E-1)$$

1088 The direct integration of the ordinary differential Eq.  
1090 (E-1) taking into account the inlet boundary condition  
1091 (Eq. (A-6)) results in the expression for the particle flux  
1092 profile

$$Q = \exp(-AX) \quad (E-2)$$

1094 which coincides with the flux profile (Eq. (C-18)) in  
1095 semi-infinite media.

1096 Substitution of the flux expression Eq. (E-2) into Eq.  
1097 (A-4) leads to a first-order ordinary differential equa-

tion for suspended concentration profile. The solution  
that takes account of the outlet boundary condition Eq.  
(A-7) is given by

$$C(X) = \frac{1}{1 + A\varepsilon_D} \left[ \exp(-AX) + A\varepsilon_D \exp\left(\frac{1}{\varepsilon_D}(X-1) - A\right) \right]. \quad (E-3)$$

The inlet concentration is calculated from Eq. (E-3):

$$C(0) = \frac{1}{1 + A\varepsilon_D} \left[ 1 + A\varepsilon_D \exp\left(-\frac{1}{\varepsilon_D} - A\right) \right] \quad (E-4)$$

The outlet concentration at  $X=1$  is also obtained di-  
rectly from Eq. (E-3):

$$C(1) = \exp(-A) \quad (E-5)$$

The outlet boundary condition (A-7) implies that the  
particle flux and the suspended concentration coincide  
at  $X=1$ .

The retention dynamics can be found from Eq. (A-3)  
using the expression for the particle flux (Eq. (E-2)):

$$S(X, T) = AT \exp(-AX) \quad (E-6)$$

## Appendix F. Travelling wave solutions

Let us find travelling wave solutions

$$C = C(w), \quad S = S(w), \quad w = X - uT \quad (F-1)$$

for system Eq. (20), where  $u$  is an unknown wave  
speed.

The corresponding system of ordinary differential  
equations as obtained from Eq. (20) is

$$\frac{dS}{dw} = -A(S)(C + S) \quad (F-2)$$

$$\frac{dC}{dw} = \frac{1}{\varepsilon_D} [(1-u)C - uS] \quad (F-3)$$

The initial condition (12) for system Eq. (20) was  
already used during integration (Eqs. (21)–(24)), so the  
dynamic system (Eqs. (F-2) and (F-3)) fulfils the  
corresponding boundary condition:

$$w \rightarrow +\infty : C \rightarrow 0 ; S \rightarrow 0 \quad (F-4)$$

The existence of the limited solution at minus infin-  
ity implies for Eq. (F-2) that  $A(S_m)=0$ , i.e. the filtration  
coefficient should be a blocking function, see Eq. (5).  
The corresponding boundary condition at minus infin-  
ity for the dynamic system (Eqs. (F-2) and (F-3)) is

1138 obtained from the boundary condition (14):

$$w \rightarrow -\infty : C \rightarrow 1; S \rightarrow S_m \quad (F-5)$$

1140 Substituting Eq. (F-5) with Eq. (F-3), we obtain the  
1142 wave speed:

$$0 < u = \frac{1}{1 + S_m} < 1 \quad (F-6)$$

1143 The wave speed (Eq. (F-6)) fulfils the Hugoniot  
1146 condition of mass balance on the shock for conserva-  
1147 tion law (Eq. (1)).

1148 The autonomous system (Eqs. (F-2) and (F-3)) can  
1149 be reduced to one ordinary differential equation with  
1150 unknown  $C = C(S)$ :

$$\frac{dC}{dS} = -\frac{(1-u)C - uS}{\varepsilon_D A(S)(C+S)} \quad (F-7)$$

1153 A phase portrait of the dynamic system (Eq. (F-7)) is  
1154 presented in Fig. 12. The analysis repeats that for the  
1155 HLL system as performed by Logan, 2000. The system  
1156 has a saddle singular point (0, 0) and an unstable  
1157 repulsive node singular point ( $S_m, 0$ ). There does  
1158 exist the unique trajectory connecting two critical  
1159 points that corresponds to the solution of the problem  
1160 (Eqs. (F-2) and (F-3)).

1161 The travelling wave solution is obtained by integrat-  
1162 ing Eq. (F-2):

$$w(S) = -\int^S \frac{1}{A(s)(C(s)+s)} ds + const. \quad (F-8)$$

1163 The solution of the initial-boundary value problem  
1166 (Eqs. (12) and (14)) tends asymptotically to the travel-  
1167 ling wave (Eqs. (F-7) and (F-8)). It happens when  $T$   
1168 tends to infinity along each characteristic  
1169  $X - uT = w = const$ :

$$\lim_{T \rightarrow \infty} C(X, T)|_{w=const} = \lim_{T \rightarrow \infty} C(w + uT, T) = C(w) \quad (F-9)$$

$$\lim_{T \rightarrow \infty} S(X, T)|_{w=const} = \lim_{T \rightarrow \infty} S(w + uT, T) = S(w) \quad (F-10)$$

1170  
1173 Following Tikhonov and Samarskii (1990), we approx-  
1174 imate the solution of the problem (Eqs. (20) (12) and  
1175 (14)) by the travelling wave for any finite  $T$ .

1176 The initial-boundary problem (Eqs. (20) (12) and  
1177 (14)) has the Goursat type and allows determination  
1178 of the retained concentration at the inlet without finding  
1179 the global solution. Fixing  $C=1$  at  $X=0$  in the retention

kinetics (Eq. (A-3)) and dividing variables in the ordi- 1180  
nary differential equation, we obtain 1181

$$X = 0 : T = \int_0^{S(0,T)} \frac{dy}{A(y)} = \Phi(S) \quad (F-11)$$

The expression for retained concentration is obtained 1182  
from Eq. (F-11) applying the inverse function 1185

$$S(0, T) = \Phi^{-1}(T) \quad (F-12)$$

The travelling wave solution is invariant with respect 1186  
to a shift  $(X, T) \rightarrow (X + const, T)$ . Let us fix the 1189  
constant  $w$  in Eq. (F-8) for each moment  $T$  in such a 1190  
way, that the inlet retained concentration is the same as 1191  
that in the solution of the initial-boundary value prob- 1192  
lem (Eq. (F-12)). So, Eq. (F-8) takes the form: 1193

$$w(S, T) = -\int_{\Phi^{-1}(T)}^S \frac{1}{A(s)(C(s)+s)} ds - uT \quad (F-13)$$

Finally, the delay term in the travelling wave variable is 1194  
chosen for any  $T$  in such a way, that the Goursat 1197  
condition (Eq. (F-12)) is fulfilled. 1198

Let us show that it provides with the total mass 1199  
balance for the conservation law (Eq. (1)). 1200

Substituting the travelling wave form (Eq. (F-1)) 1201  
into the mass balance (Eq. (A-2)) 1202

$$\int_{-uT}^{\infty} (C+S)dw = T \quad (F-14)$$

and performing integration in  $x$ , from the Eq. (F-13) 1203  
we obtain 1205

$$\begin{aligned} T &= \int_{-uT}^{\infty} (C+S)dw = \int_0^{S(-uT)} \frac{ds}{A(s)} \\ &= \Phi(S(-uT)) = \Phi(S(0, T)) \end{aligned} \quad (F-15)$$

So, the solution (Eq. (F-13)) fulfils the integral mass 1206  
balance for the domain  $0 < X < 8$ . 1209

Solution in the plane  $(X, T)$  for the retained particle 1210  
concentration can be obtained by substituting 1211  
 $w = X - uT$  into Eq. (F-13): 1212

$$X(S, T) = -\int_{\Phi^{-1}(T)}^S \frac{1}{A(s)(C(s)+s)} ds \quad (F-16)$$

Eq. (F-16) is an approximate solution for initial- 1213  
boundary value problem (Eqs. (12) and (14)). 1216



## 1217References

1218

- 1219 Bedrikovetsky, P.G., 1993. *Mathematical Theory of Oil and Gas*  
1220 *Recovery*. Kluwer Academic Publishers, Dordrecht.
- 1221 Bedrikovetsky, P.G., Marchesin, D., Checaira, F., Serra, A.L.,  
1222 Resende, E., 2001. Characterization of deep bed filtration system  
1223 from laboratory pressure drop measurements. *J. Pet. Sci. Eng.* 64,  
1224 167.
- 1225 Bedrikovetsky, P., Marchesin, D., Hime, G., Alvarez, A., Marchesin,  
1226 A.O., Siqueira, A.G., Souza, A.L.S., Shecaira, F.S., Rodrigues,  
1227 J.R., 2002. "Porous media deposition damage from injection of  
1228 water with particles." VIII Ecmor European Conference on Math-  
1229 ematics in Oil Recovery, Sept. 3–6, Austria, Leoben.
- 1230 Bolster, C.H., et al., 1998. A method for calculating bacterial depo-  
1231 sition coefficients using the fraction of bacteria recovered from  
1232 laboratory columns. *Environ. Sci. Technol.* 32, 1329.
- 1233 Danckwerts, P.V., 1953. Continuous flow systems: distribution of  
1234 residence times. *Chem. Eng. Sci.* 2, 1.
- 1235 Elimelech, M., et al., 1995. *Particle Deposition and Aggregation:*  
1236 *Measurement, Modelling, and Simulation*. Butterworth-Heine-  
1237 mann, Oxford, England.
- 1238 Ginn, T.R., 2002. A travel approach to exclusion on transport in  
1239 porous media. *Water Resour. Res.* 38, 1129.
- 1240 Grolimund, D., et al., 1998. Transport of in situ solubilized colloidal  
1241 particles in packed soil columns. *Environ. Sci. Technol.* 32, 3562.
- 1242 Harter, T., et al., 2000. Colloid transport and filtration of *Cryptospor-*  
1243 *idium parvum* in sandy soils and aquifer sediments. *Environ. Sci.*  
1244 *Technol.* 34, 62.
- 1245 Herzog, J.P., Leclerc, D.M., Goff, P.L., 1970, May. Flow of suspen-  
1246 sions through porous media — application to deep filtration. *Ind.*  
1247 *Eng. Chem.* 62 (5), 8.
- 1248 Iwasaki, T., 1937. Some notes on sand filtration. *J. Am. Water Works*  
1249 *Assoc.* 29, 1591.
- 1250 Jensen, J.L., et al., 1997. *J. Statistics for Petroleum Engineers and*  
1251 *Geoscientists*. Prentice Hall PTR, New Jersey.
- 1252 Jin, Y., et al., 1997. Sorption of viruses during flow through saturated  
1253 sand columns. *Environ. Sci. Technol.* 31, 548.
- 1254 Kampen, Van N.G., 1984. *Stochastic Processes in Physics and Chem-*  
1255 *istry*. North-Holland, Amsterdam–Oxford.
- 1256 Kechagia, P., Tsimpanogiannis, I., Yortsos, Y., et al., 2002. On the  
1257 upscaling of reaction-transport processes in porous media with  
1258 fast or finite kinetics. *Chem. Eng. Sci.* 57 (13), 2565.
- 1259 Khilar, K.C., Fogler, H.S., 1998. *Migration of Fines in Porous Media*.  
1260 Kluwer Academic Publishers, Dordrecht–Boston–London.
- 1261 Kretzschmar, R., Barmettler, K., et al., 1997. Experimental determi-  
1262 nation of colloid deposition rates and collision efficiencies in  
1263 natural porous media. *Water Resour. Res.* 33, 1129.
- 1264 Kuhnen, F., Barmettler, K., et al., 2000. Transport of iron oxide  
1265 colloids in packed quartz sand media. *J. Colloid Interface Sci.*  
1266 231.
- 1267 Lake, L.W., 1989. *Enhanced Oil Recovery*. Prentice Hall, Englewood  
1268 Cliffs.
- 1269 Landau, L.D., Lifshitz, E.M., 1987. *Fluid mechanics*. (2nd ed.).  
1270 *Course of Theoretical Physics*, vol. 6. Pergamon Press, Oxford.
- 1271 Logan, D.J., 2001. *Transport Modeling in Hydrogeochemical Sys-*  
1272 *tems*. Springer.
- 1273 Massei, N., et al., 2002. Transport of particulate material and dis-  
1274 solved tracer in a highly permeable porous medium: comparison  
1275 of the transfer parameters. *J. Contam. Hydrol.* 57, 21.
- 1276 Nikolaevskij, V.N., 1990. *Mechanics of Porous and Fractured Media*.  
1277 World Scientific, New Jersey–Hong Kong.
- 1278 Pang, S., Sharma, M.M., 1994. A model for predicting injectivity  
1279 decline in water injection wells. SPE paper 28489 presented at  
1280 69th Annual Technical Conference and Exhibition held in New  
1281 Orleans, LA, 25–28 September.
- 1282 Payatakes, A.C., et al., 1974. Application of porous medium models  
1283 to the study of deep bed filtration. *Can. J. Chem. Eng.* 52, 727.
- 1284 Polyanin, A.D., 2002. *Handbook on linear partial differential equa-*  
1285 *tions for scientists and engineers*. Chapman and Hall CRC Press,  
1286 Boca Raton–London.
- 1287 Santos, A., Bedrikovetsky, P., 2005. Size exclusion during particle  
1288 suspension transport in porous media: stochastic and averaged  
1289 equations. *J. Comput. Appl. Math.* 3.
- 1290 Sharma, M.M., Yortsos, Y.C., 1987a. Transport of particulate suspen-  
1291 sions in porous media: model formulation. *AIChE J.* 33 (10),  
1292 1636.
- 1293 Sharma, M.M., Yortsos, Y.C., 1987b. A network model for deep bed  
1294 filtration processes. *AIChE J.* 33 (10), 1644–1653.
- 1295 Sharma, M.M., Yortsos, Y.C., 1987c. Fines migration in porous  
1296 media. *AIChE J.* 33 (10), 1654–1662.
- 1297 Sorbie, K., 1991. *Polymer-improved Oil Recovery*. CRC Press, Boca  
1298 Raton–London.
- 1299 Tiab, D., Donaldson, E.C., 1996. *Petrophysics*. Gulf Publishing,  
1300 Houston.
- 1301 Tikhonov, A.N., Samarskii, A.A., 1990. *Equations of Mathematical*  
1302 *Physics*. Dover, New York.
- 1303 Tufenkji, N., et al., 2003. Interpreting deposition patterns of microbial  
1304 particles in laboratory-scale column experiments. *Environ. Sci.*  
1305 *Technol.* 37, 616.
- 1306 Unice, K.M., Logan, B.E., 2000. Insignificant role of hydrodynamic  
1307 dispersion on bacterial transport. *J. Environ. Eng.* 126, 491.
- 1308 van Genuchten, Th.W., 1981. Analytical solutions for chemical trans-  
1309 port with simultaneous adsorption, zero-order production and  
1310 first-order decay. *J. Hydrol.* 49, 213.
- 1311 Wennberg, K.E., Sharma, M.M., 1997. Determination of the filtration  
1312 coefficient and the transition time for water injection. *Proceedings*  
1313 *of the SPE European Formation Damage Conference*, SPE 38181,  
1314 The Hague, The Netherlands, June 2–3.

1315